

Exploring the CO₂ fugacity along the east coast of South America aboard the schooner *Tara*

Léa Olivier^{1,2}, Jacqueline Boutin², Gilles Reverdin², Christopher Hunt³, Thomas Linkowski⁴, Alison Chase^{5,6}, Nils Haentjens⁶, Pedro C. Junger^{7,8*}, Stéphane Pesant⁹, & Douglas Vandemark³

¹Alfred Wegener Institute, Helmholtz Centre for Polar and Marine Research, Bremerhaven, Germany
²LOCEAN-IPSL, Sorbonne Université-CNRS-IRD-MNHN, Paris, France
³OPAL, EOS, University of New Hampshire, Durham, New Hampshire, USA
⁴Fondation Tara Ocean
⁵Applied Physics Laboratory, University of Washington, Seattle, Washington
⁶School of Marine Sciences, University of Maine, Orono, Maine
⁷Department of Hydrobiology, Universidade Federal de São Carlos (UFSCar), São Carlos, SP 13565-905, Brazil
⁸Programa de Pós-Graduação em Ecologia e Recursos Naturais, Centro de Ciências Biológicas e da Saúde, Universidade Federal de São Carlos (UFSCar), São Carlos, SP 13565-905, Brazil
⁹European Molecular Biology Laboratory, European Bioinformatics Institute, Wellcome Genome Campus, Hinxton, Cambridge CB10 1SD, United Kingdom
*Present address: Institut de Biologie de l'École Normale Supérieure (IBENS), École Normale Supérieure, CNRS, INSERM, PSL Université Paris, Paris 75005, France.

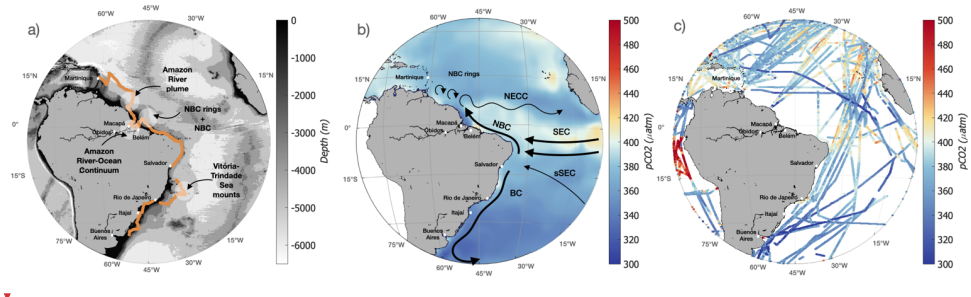
Correspondence to: Léa Olivier (lea.olivier@awi.de)

Abstract. The air-sea CO₂ flux in the coastal ocean is a **critical** component of the global carbon budget, **yet it remains poorly understood** due to **limited** data, the many sources and sinks of carbon and their complex interactions. In **August-November** 2021, the *Tara* schooner collected **over** 14,000 km of CO₂ fugacity (fCO₂) measurements along the coast of South America, including in the Amazon River-Ocean continuum (<https://doi.org/10.5281/zenodo.13790064>, Olivier et al., 2024a). The Amazon River and its oceanic plume **exhibit** complex **interactions**, under a combined influence of many processes such as tides and bathymetry. **Observations revealed a wide range of fCO₂ values, from up to up to 3000 µatm in the river to a minimum of 42 µatm downstream of the plume, where values were notably lower than atmospheric levels.** South of the estuary, the **fCO₂** of the North Brazil **Current's waters (0-9°S) exceeds 400 µatm, while along the Brazil Current (10-30°S), fCO₂ is around 400 µatm and decreases with temperature and distance from the equator. Due to its high variability in coastal environment, in the dataset salinity emerged as the primary driver of fCO₂ variability across this dynamic region.** Despite strong variability, comparison with discrete samples of other carbonate parameters **showed a mean difference of 2 µatm**, within the range of uncertainties **of the chemical formulas** used for comparison. This **dataset provides critical insights into** the under-sampled region of the Brazilian coast, **improving our understanding of coastal fCO₂ dynamics and their role in the global carbon budget.**

- a supprimé: key
- a supprimé: . However,
- a supprimé: the scarcity of
- a supprimé: in these waters remain poorly understood.
- a supprimé: interactions between the
- a supprimé: are
- a supprimé: , and
- a supprimé: Downstream of the Amazon River plume, the
- a supprimé: is low compared with that of the atmosphere, reaching a minimum of 42 µatm. In the river, fCO₂ reaches
- a supprimé: .
- a supprimé: waters
- a mis en forme : Indice
- a supprimé: Current have a fCO₂ exceeding
- a supprimé: . Along
- a supprimé: .
- a supprimé: , as does
- a supprimé: , as the schooner sails away
- a supprimé: Nevertheless, in all the data collected in this
- a supprimé: varies greatly, and therefore describes best the variability ...
- a supprimé: .
- a supprimé: the
- a supprimé: and uncertainties in the data
- a supprimé: shows that the
- a supprimé: differences (
- a supprimé:) are
- a supprimé: related to
- a supprimé: formula
- a supprimé: the
- a supprimé: data set helps to fill the gap in our knowledge of the behavior of fCO₂ in

65 **1 Introduction**

The global ocean is a sink that absorbs 26% of the anthropogenic carbon dioxide (CO₂) emitted into the atmosphere by the burning of fossil fuels and land use change (Friedlingstein et al., 2023). While the ocean participates in mitigating the effects of climate change by storing both heat and CO₂, it is also subject to profound changes such as ocean warming and acidification. Coastal and marginal oceans play a pivotal role in the global carbon cycle by connecting terrestrial, oceanic and atmospheric carbon reservoirs. The air-sea CO₂ flux varies spatially over the world's oceans, and some of the strongest gradients are found in the coastal regions (Landschützer et al., 2020). These regions present much higher temporal and spatial variability compared to the open ocean (Borges, 2005; Cai et al., 2006; Laruelle et al., 2014; Roobaert et al., 2019). Recent studies estimate that the uptake of CO₂ per unit area is even greater over continental shelf seas than over the open ocean due to the contribution of the arctic shelves and the impact of rivers (Chen et al., 2013; Laruelle et al., 2014; Roobaert et al., 2019). Despite the fact that coastal waters play a major role in the livelihood of humans, and are strongly affected by human activities, our understanding of these waters is strongly limited by the low number of observations (Bauer et al., 2013).



80 **Figure 1: a) Bathymetry of the Atlantic Ocean (ETOPO2v2) and journey of the schooner Tara (orange line). b) 1998-2015 September climatology of the partial pressure of CO₂ (pCO₂, Landschützer et al., 2020), the black arrows represent some of the main surface geostrophic currents in boreal fall. c) pCO₂ along the ship trajectories in August-September-October (SOCAT, data from 1957 to 2022). NBC: North Brazil Current, NECC: North Equatorial Counter Current, SEC: South Equatorial Current, sSEC: southern branch of the SEC, BC: Brazil Current.**

While the coastal and marginal seas of the mid and northern latitudes are sinks of CO₂ with regards to the atmosphere, the tropical coastal oceans act as sources (Cai et al., 2006; Laruelle et al., 2014; Takahashi et al., 2002). There are several reasons for this, including the reduced solubility of CO₂ at high temperatures, and the upwelling of deep waters rich in dissolved inorganic carbon (DIC) in the equatorial upwelling and along the coast (Andrié et al., 1986; Takahashi et al., 2002). This has also been observed on regional studies, and one region presenting a strong and heterogeneous signal is the western tropical Atlantic coastal ocean (Lefèvre et al., 2017; Lefèvre et al., 2010; Olivier et al., 2022).

One example is the Amazon river-ocean continuum (AROC). It represents one of the greatest environmental gradients on the interface between land and ocean in the world (eg. Araujo et al., 2017). The Amazon River system discharge is unique in the

a supprimé:

a supprimé :

a supprimé: It represents one of the greatest environmental gradients on land and ocean in the world.

95 global ocean. It contributes as much freshwater as the next seven largest rivers combined, accounting for 20% of the global
 riverine freshwater input to the ocean (Dai and Trenberth, 2002). The resulting Amazon River plume (ARP) spreads across up
 to 1.3 million km² of the tropical Atlantic Ocean and creates a significant CO₂ sink relative to the atmosphere, primarily driven
 by strong biological drawdown (Cooley et al., 2007; Körtzinger, 2003; Subramaniam et al., 2008). combined with low salinities
 (Ibáñez et al., 2016; Lefèvre et al., 2010). Opposing this, the Amazon River releases almost as much CO₂ into the atmosphere
 100 annually as the rainforest absorbs (Richey et al., 2002; Sawakuchi et al., 2017). The main source of CO₂ in the river comes
 from the breakdown of young organic carbon from the land by microbes (Mayorga et al., 2005; Ward et al., 2013, 2015). The
 lower Amazon River (from Óbidos to the river mouth) releases an amount of CO₂ slightly higher (0.02 Pg C yr⁻¹, Sawakuchi
 et al., 2017) than the uptake by the ARP in the Atlantic Ocean (0.014 Pg C yr⁻¹, Körtzinger, 2003). Sawakuchi et al. (2017)
 demonstrated the importance of quantifying CO₂ fluxes in the lower Amazon by adding the Óbidos-Macapá section to the
 105 Amazon River budget. On the other hand, oceanographic studies, carried out in particular during the ANACONDAS (in 2011,
2012 and 2013, Mu et al., 2021) and Camadas Finas III (October 2012, Araujo et al., 2017) campaigns, focused on the ARP
development, maximum extension and early decay have shown the extent of CO₂ undersaturation in the ARP. However, the
estuary, which is the link between these two systems is little known, if at all (Sawakuchi et al., 2017; Ward et al., 2017).
Valerio et al., (2018) collected discrete samples for CO₂ partial pressure all the way to the river mouth in April 2017 but do
 110 not address the Amazon River CO₂ flux budget. Chen et al. (2013) studied the CO₂ in the world's coastal seas by evaluating
the air-sea exchanges of CO₂ in 165 estuaries, but no data were available in the Amazon estuary, despite being arguably one
with the strongest impact. Since then, Araujo et al., (2017) collected discrete DIC and total alkalinity (TA) samples at the
mouth of the Pará-Tocantins River system, near the town of Belém.

115 The Brazilian continental shelf hosts diverse CO₂ flux dynamics influenced by regional oceanographic and biogeochemical
processes. The ARP plays a key role in air-sea CO₂ exchange, with strong seasonal variability driven by river discharge,
biological productivity, and salinity gradients (eg. Lefèvre et al., 2010; Mu et al., 2021; Olivier et al., 2024b). In the North
Brazil Current (NBC) region, upwelling and mesoscale eddies contribute to CO₂ flux variability, modulating carbon exchange
between the ocean and atmosphere (eg. Monteiro et al., 2022; Olivier et al., 2022). Further south, the Vitória-Trindade
 120 Seamount Chain interacts with regional currents (Napolitano et al., 2021), influencing nutrient transport and biological activity
that can affect CO₂ fluxes. The Lagoa dos Patos and Guanabara Bay are important estuarine systems where terrestrial carbon
inputs, tidal mixing, and anthropogenic influences create spatially and temporally variable CO₂ flux patterns (Cotovicz Jr et
al., 2015). Along the broader Brazilian continental shelf, complex interactions between ocean circulation, biological
productivity, and local conditions shape regional carbon dynamics, making in situ observations critical for understanding these
 125 fluxes.

While data gaps in the open ocean have begun to narrow, partly due to advancements such as the Argo biogeochemical float
 program, it is not the case for biogeochemical measurement on the shelves and continental margins. Continuous surface

a supprimé: . Opposing this, the Amazon River outgasses nearly as much CO₂ as the rainforest sequesters on an annual basis.

a supprimé: On the other hand, oceanographic studies, carried out in particular during the ANACONDAS (Mu et al., 2021)

a supprimé: (Araujo et al., 2017) campaigns, have shown the extent of CO₂ undersaturation in the ARP. However,

a supprimé: . Chen et al. (2013) extensively

a mis en forme : Français

a supprimé: Since then, only discrete samples of DIC and total alkalinity (TA) have been taken at the mouth of the Pará-Tocantins River system, near the town of Belém (Araujo et al., 2017).

a supprimé: While the data gap

a supprimé: has slowly started to be filled up by the development of...

a supprimé: This is also not the case for the continuous

fugacity of CO₂ (fCO₂) measurements carried out on ships, remain the most accurate way to assess CO₂ fluxes and are still too sparse. A notable trend in recent years is the global decline in ship-based CO₂ observations being added to the Surface Ocean CO₂ Atlas (SOCAT) database (Bakker et al., 2016), particularly since 2017 (Friedlingstein et al., 2023), mainly due to reduced funding (Dong et al., 2024). Despite recent contributions documented in publicly available open-access data, the Brazilian continental margins remain notably under-sampled, with an acute lack of data during specific seasons, such as from August to November (Fig. 1c). Recently, sailboats have provided interesting opportunities to measure CO₂ in conditions different from traditional research vessels, as highlighted by the contribution of data from racing sailboats (Landschützer et al., 2023).

a supprimé : Despite

a supprimé : sampling, as reported by

a supprimé : CO₂

a supprimé : the continental margins off Brazil are lacking in data, and even more notably when considering a particular season, such as from August to November (Fig. 1c). The number of data being added to SOCAT is also decreasing significantly since 2017 (Friedlingstein et al., 2023).

Here, we present a new fCO₂ data set, acquired on the research schooner *Tara*. This is the first time that a sailboat has been equipped with a fCO₂ equilibrator-system, which is more accurate than the membrane system used on racing yachts, but larger and more maintenance-intensive. One of the special features of the missions aboard *Tara* is the combination of physical, biogeochemical, and biological oceanography to provide comprehensive knowledge of the ocean (Bork et al., 2015; Pesant et al., 2015). Tara missions have a unique design, they are continuous for a multi-year duration, with scientists and sailors taking turns on-board. This novel dataset presents 14,000 km of fCO₂ measurements over 98 days between August to end of November 2021, primarily along the South American coast, and marking the first repeated sampling of the AROC. The cruise took place in a period of decreasing river outflow, following one of the largest Amazon flood events on record. Freshwater transport was strongly directed toward the Caribbean, with comparatively less Amazon-derived freshwater reaching the NECC and central Atlantic (Olivier et al., 2024b). It also includes measurements in the ARP and in different areas off Brazil: in the North Brazil Current (NBC), the Brazil Current, the Guanabara Bay (Rio de Janeiro), the Vitória-Trindade Sea mounts and the shelves of South Brazil, filling some of the gaps in the current data.

a supprimé : Tara missions are unique in that they are continuous for a multi-year duration, with scientists and sailors taking turns on-board. This novel dataset presents 14,000 km of fCO₂ data mostly along the coasts of South America, from August to December 2021, for the first-time sampling the AROC multiple times. It also includes measurements in the ARP and in different areas off Brazil: in the North Brazil Current (NBC), the Brazil Current, the Guanabara Bay (Rio de Janeiro), the Vitória-Trindade Sea mounts and the shelves of South Brazil, filling some of the gaps in the current data.

The primary objective of this study is to present the fCO₂ dataset acquired by *Tara*, and shed light on some of the lesser studied areas of the Amazon River, estuary and plume. Section 2 provides a detailed description of the fCO₂ measurement system, the challenges encountered during its installation on the schooner, the solutions implemented, and the validation of the dataset. Section 3 illustrates the dataset, first encompassing the whole transect and then focusing on the case study of the river-ocean continuum. Section 4 discusses possible uses of the data and the performance of the system.

a supprimé :

2 Instruments and methodology

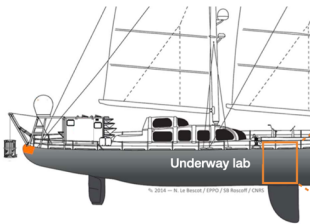
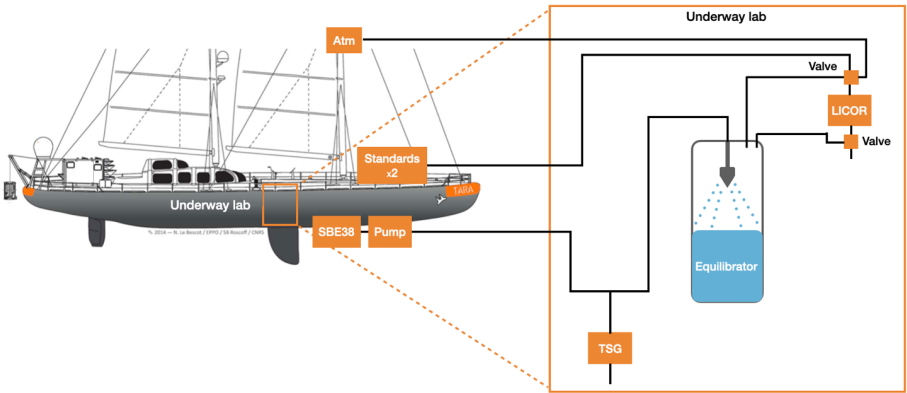
2.1. Mission Microbiomes AtlantECO

For two years, the schooner *Tara* sailed 70,000 kilometers across the South Atlantic Ocean to study the ocean microbiome and its interactions with climate and pollution. The 36 m long schooner is equipped with numerous scientific equipment operated by a team of four to six scientists and six sailors consistently on board. During the first part of the Mission Microbiomes AtlantECO, the schooner sampled the entire east coast of South America, from August to end of November 2021 (Fig. 1a).

a supprimé :

and 45 seconds, depending on flow rate (Pierrot et al., 2009). Unlike a traditional research vessel (RV), space and time for maintenance are limited on board the schooner. The continuous water line is used by 9 instruments, stored under in the fore hold, and in a small laboratory of a 2.5 m^2 . The installation of the CO₂ system required some compromises chosen with the help from the sailors and engineers on board, to fit with the schooner constraints and to limit the loss in measurement accuracy (originally of less than $2\text{ }\mu\text{atm}$). We will detail the modifications in the setup of the fCO₂ system, and then discuss the accuracy of the data obtained, before illustrating the large variability of the sampled area.

a supprimé: few square meters.



a supprimé:

Figure 2: Schematic of the underway laboratory and fCO₂ system onboard the schooner *Tara*, adapted from (Pesant et al., 2015).

Seawater enters through the hull at less than 1.5 m depth where a Sea Bird Electronics (SBE) 38 temperature sensor is located for an accurate measurement of sea surface temperature (SST). It then enters a debubbler to remove most of the bubbles that can be caused by such shallow water intake, especially in rough seas, and goes through a large particles filter. The seawater circuit is then split into two to feed the many underway instruments. One branch first flows through a thermosalinograph (TSG, SBE 45) to measure temperature and salinity (temperature accuracy of $\pm 0.002\text{ }^{\circ}\text{C}$, conductivity accuracy of $\pm 0.0003\text{ S m}^{-1}$). The other branch first flows into the equilibrator of the fCO₂ system after less than 5 m of tubing, at a rate of $2\text{--}6\text{ L min}^{-1}$. We make the hypothesis that at this high flow rate and short path, the temperature is similar in the equilibrator and in the TSG, as both instruments are first in their respective water circuit and at a similar distance from the split. We suspect that this choice introduces less uncertainty than directly using SST (action recommended for missing equilibrator temperature data, Pierrot et al., 2009), although we do not have the data to fully validate this hypothesis. Fortunately, the sailboat is small compared to an open ocean RV, so the pipe length from the hull to the underway instruments is considerably smaller and the temperature difference between the hull sensor (SBE38) and the TSG is small (always below $0.1\text{ }^{\circ}\text{C}$ averaging $0.07\text{ }^{\circ}\text{C}$, Figure 2).

a supprimé: .

a supprimé: first

a supprimé: accurately

a supprimé: using

a supprimé: 5

245 The fCO₂ system uses a shower spray air–sea equilibrator of 2.5 L as described by Dickinson, (2007) and used by Vandemark
et al., (2011). Water is sprayed or trickled inside a chamber, creating a large surface area for rapid equilibration with the
headspace air. A closed loop of air flows through the equilibrator where the air-water exchanges happen, the equilibrated air
is drawn at 100 mL/min through tubing containing a Nafion selectively permeable membrane with a counterflowing stream of
dry nitrogen to remove water vapor from the sample gas stream. It is then sent to a non-dispersive infrared CO₂ analyzer, a
250 LICOR LI-840A. It detects the molar fraction of CO₂ (xCO₂) in dry air by infrared detection, from which fCO₂ is computed
following Henry’s law (detailed in the annex of Pierrot et al., 2009). Ideally, the computation requires the pressure inside the
equilibrator. The equilibrator was not equipped with a pressure sensor, but was designed to be at atmospheric pressure.
Atmospheric pressure was measured by a Vaisala Barometer PTB100 with an accuracy of ± 0.3 hPa at 20°C at the rear of the
ship. A temperature correction to the seawater fCO₂ data is applied based on the difference between the temperature sensor in
255 the hull and the TSG.

Through a system of electro-valves, four circuits are operated, one for the atmospheric air, one for each of the two reference
gases, and one for the air equilibrated with seawater. The atmospheric air intake is located on the first cross tree of the schooner
front mast (~ 10 m). The two 20 L reference gases tanks of 0 ppm and 502.3 ppm are stored on the front deck. These values
were chosen because they effectively bracket the range of oceanic fCO₂ values in this highly variable environment,
260 encompassing most of the observed data except in the river. As a result, fCO₂ values above 500 µatm are more uncertain and
should be interpreted with caution. The number of different calibration gases was reduced from 4 (on a traditional RV) to 2
(as done on racing sailboats, Landschützer et al., 2023). The reduced use of standards results from complications to replace
the gas cylinders abroad (especially during the covid period), as well as to store them onboard. It is recommended to measure
a complete set of standards every 3 hours. During the first week, to test the system, a complete set of standards and atmospheric
265 cycle was measured for 15 minutes every hour. As the system behaved well and the drift of the LICOR was acceptable (less
than 0.4 ppm over 6 hours), the measurement of standards was changed to every 6 hours (on 31/08), then to every 12 hours
(on 02/09) to save the reference gases. Although not ideal, this is still more frequent than the once-a-day rate on the racing
sailboats (Landschützer et al., 2023).

It is quite challenging to install such a system on a schooner, but it also presents numerous advantages, one of the most
270 important being the shallow depth of the seawater intake. Tara’s seawater intake is located below the hull, at 1.5 m depth. This
is shallower than on many research vessels (5 m depth on average), and better represents the actual air-sea exchanges,
especially in stratified regions (Ho and Schanze, 2020). The system also has the advantage to be able to work in turbid
environment. The equilibrator was cleaned at each stopover, and each time the ship exited a major river (so 7 times in total) to
avoid the buildup of mud, and the system therefore recorded data during the whole time spent in the Amazon River.

a supprimé: (
a supprimé: ;
a supprimé: .
a supprimé: then dried and
a supprimé: the

a supprimé: , detailed in Annex

a supprimé: air equilibrated with seawater
a supprimé: atmospheric air
a supprimé: ¶

a supprimé: increased
a supprimé: ,

a supprimé: regularly

275 2.3. Using atmospheric CO₂ to validate the span value

It is customary to measure in the laboratory the value of each non-zero standard after the cruise as its value can differ from the
value reported by the constructor. Unfortunately, this was not possible because after this long cruise (and some gas leakage in

rough seas) the tank was empty. The value requested for the non-zero standard was 500 ppm, with a reported 507.9 ppm value by the supplier (Airgas), with an uncertainty of 2 %. The value measured in the laboratory before the cruise was 530 ppm. However, we found that choosing this value of 530 ppm results in unrealistically high atmospheric (close to 440 ppm) and oceanic (> 450 ppm) xCO₂ measurements (blue in Fig. 3). Furthermore, it is outside of the uncertainty range reported by the manufacturer.

295

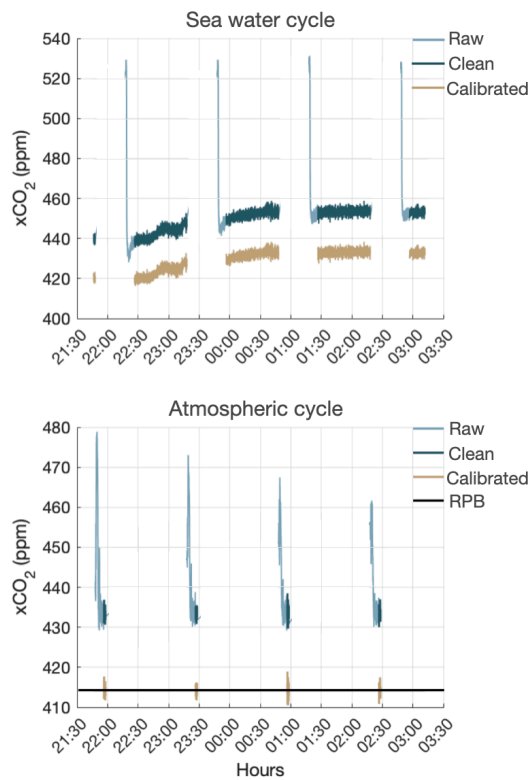


Figure 3: Time-series of *Tara* xCO₂ extracted near Barbados (night of 18-19 August 2021) for the seawater cycle (top) and atmospheric cycle (bottom). The raw data are shown in light blue, the data cleaned for valve change pollution in dark blue and the clean and calibrated data in **light** brown. For the atmospheric cycle, the value measured at Ragged Point, Barbados (RPB) on 15 August 2021 (414.15 ppm) is shown in black.

300

To address this calibration issue, we take advantage of the atmospheric xCO₂ measured on board. A few days after departure, during the night from 18 to 19 August 2021, *Tara* sailed in close vicinity to the Island of Barbados, where recurrent accurate measurements of atmospheric xCO₂ are taken at Ragged Point, Barbados (RPB). The xCO₂ measured by *Tara* calibrated using the value of 530 ppm for the span was very stable over 4 hours at 437.09 ppm. The atmospheric xCO₂ measured at RPB on 15 August 2021 (closest measure to *Tara*'s passage) was 414.245 ppm. In order for the *Tara* xCO₂ data near Barbados to match the ones at RPB, the span value should be 502.3 ppm, which is within the uncertainty range provided by Airgas. This span value was then used to calibrate the entire dataset (light brown in Fig. 3). This approach assumes that the atmospheric CO₂ near Barbados is representative of the value on *Tara*. During the time *Tara* was near the island, winds were moderate and blowing from the sea (not shown), so the atmospheric xCO₂ at RPB is not expected to vary much from day to day (~ 0.5 ppm). In the worst case, an error of 1 ppm in the calibration value would lead to a ± 0.84 ppm averaged difference over the dataset. *Tara* crossed highly variable regions during its voyage, supporting our confidence that the uncertainty on the dataset due to this span value is not significantly impacting the results.

a supprimé: 19

a supprimé: 20

a supprimé: yellow

a supprimé: method

2.3. Validation of the dataset

Samples of TA and DIC were taken at each station. Out of a total of 78 samples, 17 are from the surface (Metzl et al., 2024). Samples were drawn from the rosette into 0.5 L borosilicate glass bottles, ensuring minimal air contamination, and immediately poisoned with 400 µL of mercuric chloride (HgCl₂) to prevent biological alteration. TA was measured using open-cell titration with a hydrochloric acid titrant, while DIC was analyzed using acidification followed by CO₂ extraction and detection via infrared or coulometric methods. Quality control was ensured through calibration with certified reference materials to maintain an accuracy of ±4 µmol kg⁻¹ (Metzl et al., 2024). Their salinity ranges on a salinity scale from 0 inside the Amazon River to 37.3 in the North Brazil Current. The fCO₂ is computed from the near-surface ocean DIC and TA using the CO2SYS v3.1 software (Sharp et al., 2020) to compare with the continuous fCO₂ measurements (Fig. 4). The dissociation constants were taken as the one of Mehrbach refitted by Dickson and Millero (Dickson and Millero, 1987; Mehrbach et al., 1973) and nutrients were neglected. The dissociation constants used are the same as those in Lefevre et al. (2010) to ensure consistency for comparison in Section 4. However, we also tested several other sets of constants for additional analysis, detailed below. It is worth noting that DIC and TA is not the most accurate pair to determine the fCO₂, and it can lead to a probable error of 5.7 µatm (Millero et al., 1995).

a supprimé: Their salinity ranges on a salinity scale from 0 inside the Amazon River to 37.3 in the North Brazil Current.

a supprimé: software to compare with the continuous fCO₂ measurements (Fig.

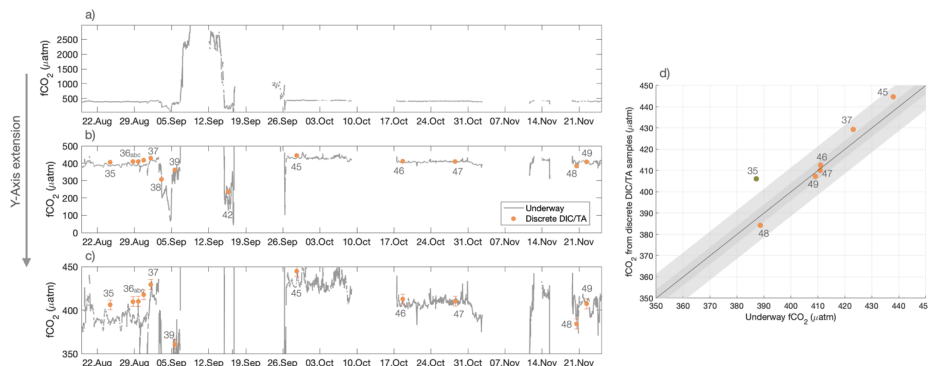
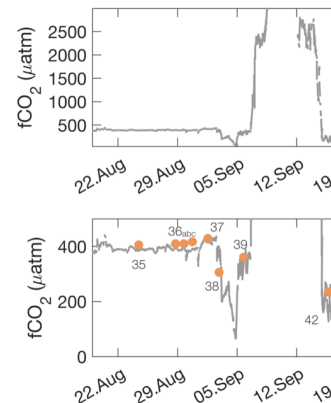


Figure 4: Time-series of the surface $f\text{CO}_2$ from 18/08/2021 to 25/11/2021, for the full range of values (a) for only oceanic values (b) for values between 350 and 450 μatm (c). The dots indicate the $f\text{CO}_2$ inferred from the DIC/TA water samples for stations 35 to 49, with error bars of 5.7 μatm to represent the uncertainty of the chemical formulas. Scatter plot of the underway $f\text{CO}_2$ and the $f\text{CO}_2$ inferred from the DIC/TA samples, for $f\text{CO}_2$ values ranging between 350 and 450 μatm . The green dot indicates a salinity difference between the CTD sensor and the sample from bottle of more than 0.5. The $f\text{CO}_2$ system was measuring the standards and not seawater during stations 36abc and 39, so these stations are not represented in (d).

Considering the compromise on accuracy that had to be made to be able to sample on the schooner, the continuous $f\text{CO}_2$ compares well to the one computed from the samples, especially after 26 September. Before that, the DIC/TA samples from the rosette during CTD casts were often taken in the presence of salinity-stratification near the surface in the ARP. The depth actually sampled for these samples is likely to be a bit deeper (by a couple of meters) than the depth of the in-line TSG (sampling depth at 1.5 m), which could explain why the $f\text{CO}_2$ measured underway is lower than the one inferred from DIC/TA in the ARP. For station 35, the difference of salinity of 0.9 between the salinity sample from the Niskin bottle and the CTD sensor is an indication of the high temporal and spatial variability of the area. Over the whole time-series no constant bias is identified, and the mean difference after 26 September is of 2.02 μatm (standard deviation of the difference (STD_{diff}) = 7.4 μatm), and drops to 0.97 μatm (STD_{diff} = 0.5 μatm) after 10 October. These results vary but remain in the same order of magnitude when changing the dissociation constants. Using constants from Lueker et al., (2000) leads to similar results (mean difference of 1.2 μatm), the largest differences are obtained using the constants from Waters et al., (2014), that are designed for a large salinity range (0-50). It improves the comparison for low salinities (before September 26) but gives slightly larger differences for high salinities (mean difference after 26 September of 0.5 μatm and 3.4 μatm after 10 October). Overall, the mean difference remains around 2 μatm , providing a reasonable estimate of the dataset's uncertainty. In the river, where $f\text{CO}_2$ values fall outside the range of the standard gas used and no discrete samples are available for direct comparison, the uncertainty is likely higher. However, the values obtained align with expected ranges for this part of the river, based on discrete samples collected in April 2017 by Valerio et al. (2018), despite differences in season and year.



a supprimé:

a supprimé: . The lower panel focuses on a smaller

a supprimé: $f\text{CO}_2$

a supprimé: .

a supprimé: the

a supprimé: .

a supprimé: very

a supprimé: stay

a supprimé:

a supprimé: an

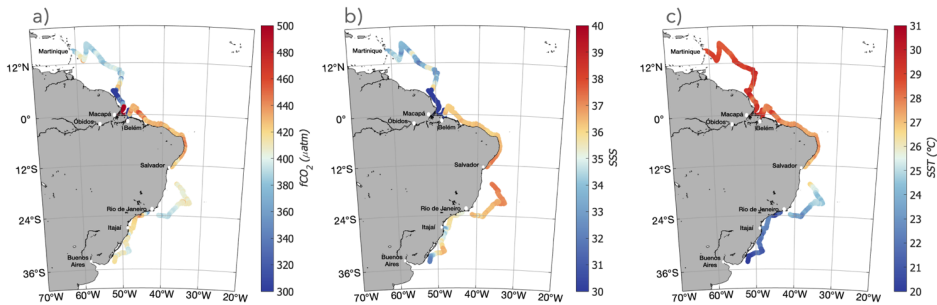
As no simultaneous dataset can be used to cross-quality check the data, the good agreement between $f\text{CO}_2$ estimated from the samples and the continuous $f\text{CO}_2$ measurements is quite important, and the mean differences are in the range of uncertainties related to inferring $f\text{CO}_2$ from the DIC and TA measurements.

2.5. Reported data

375 Following the recommendations of Pierrot et al. (2009) and of SOCAT, the dataset provides for each location and time step
the measured data: molar fraction of CO_2 in the equilibrator ($x\text{CO}_{2\text{eq}}$), sea surface salinity (SSS), temperatures (SST and T_{eq}),
and pressure (P_{atm}), the calculated variables ($p\text{CO}_{2\text{sw}}$, $f\text{CO}_{2\text{sw}}$). The atmospheric $f\text{CO}_2$ is not included as the atmospheric $x\text{CO}_2$
380 was used as a standard and for validation of the dataset. The dataset will be submitted to the 2025 SOCAT version, with
probably a flag C, as only one non-zero reference gas is used to calibrate the measured $x\text{CO}_2$. In the meantime, the data are
available in the following public repository: <https://zenodo.org/records/13790065> (Olivier et al., 2024a). In the dataset,
ancillary data are added (wind speed at 10 m, bottom depth from ETOPO2v2) to achieve a more detailed interpretation of the
data. The wind speed was measured by a Gill anemometer at the top of the mast (27 m), and then adjusted to 10 m using a
logarithmic relationship (Tennekes, 1973). This dataset addresses the overall lack of data identified by SOCAT, by covering
diverse environmental gradients with a high-resolution sampling. The use of the schooner highlights the potential of non-
385 traditional platforms for collecting high-quality data in challenging environments, complementing traditional research vessels.

3 Overview of the data

3.1. From the Caribbean to Uruguay



390 **Figure 5:** Along track a) CO_2 fugacity (complete range of values shown in Figure 4), b) sea surface salinity and c) sea surface temperature.

a supprimé: other

a déplacé (et inséré) [1]

a déplacé (et inséré) [2]

a supprimé:), and ancillary data (wind speed at 10 m).

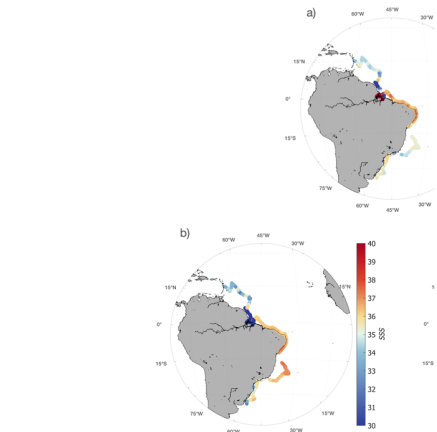
Code de champ modifié

a déplacé vers le haut [1]: The atmospheric $f\text{CO}_2$ is not included as the atmospheric $x\text{CO}_2$ was used as a standard and for validation of the dataset.

a déplacé vers le haut [2]: a flag C, as only one non-zero reference gas is used to calibrate the measured $x\text{CO}_2$. In the meantime, the data are available in the following public repository: <https://zenodo.org/records/13790065> (Olivier et al., 2024a).

a supprimé: The dataset will be submitted to the 2025 SOCAT version, with

a mis en forme : Police :Non Italique



a supprimé:

After leaving Martinique Island on 18 August 2021, *Tara* sampled the Northwestern tropical Atlantic. Surface waters exhibited strong spatial variability, with temperatures and salinities changing from 27.5 °C to 30.5°C and from 31.5 to 35.5. It induced a variability of the surface fCO₂, that ranged from 370 to 420 µatm (Fig. 5 and 6).

The schooner then crossed the salty (36) water of the NBC retroflection, before sampling the river plume that had been recently transported from the Amazon estuary. Around this period of time, the ARP was located almost entirely on the shelf as salinities lower than 30 were observed at depths shallower than 100 m (Fig. 6). The ARP water is drastically different from the one of the NBC retroflection, and the two water masses are separated by strong horizontal fronts. On 3 September 2021 *Tara* crossed a front of 14.2 in salinity between 00h30 and 5h00. This first strong front was followed by several others, on 4 September between 00h and 20h (loss of 14 salinity unit), between 4 September 20h and 5 September 9h (increase of 17 salinity unit), and finally on the 6 September between 10h and 23h the salinity dropped from 24.2 to 0 as the schooner reached the Amazon River. These sharp salinity fronts are associated with variations of temperature (variability of 2-3°C) and mainly fCO₂. In the ARP, the fCO₂ variations follow the ones in salinity. The fCO₂ of the ARP is extremely low, as for a salinity of 11 on 4 September a fCO₂ of 65 µatm is observed (Fig. 6). The salinity and fCO₂ increase on 5 September are associated with a decrease of SST, which could suggest an event of vertical mixing or local upwelling. This event generated fCO₂ fluctuations, and then as the schooner approaches the river and the salinity decreases, the conditions are switching from marine to riverine and fCO₂ rapidly increases. In the Amazon River, fCO₂ is very high, reaching 3000 µatm in Macapá.

a supprimé: samples

a supprimé: exhibit

a supprimé: salinities and

a supprimé: 31.5 to 35.5 and from

a supprimé: .

a supprimé: reflects on the

a supprimé: ranges

a supprimé: crosses

a supprimé: saline

a supprimé: water of

a supprimé: recent ARP.

a supprimé: is

a supprimé: are

a supprimé: crosses

a supprimé: is

a supprimé: drops

a supprimé: maritime

a supprimé:

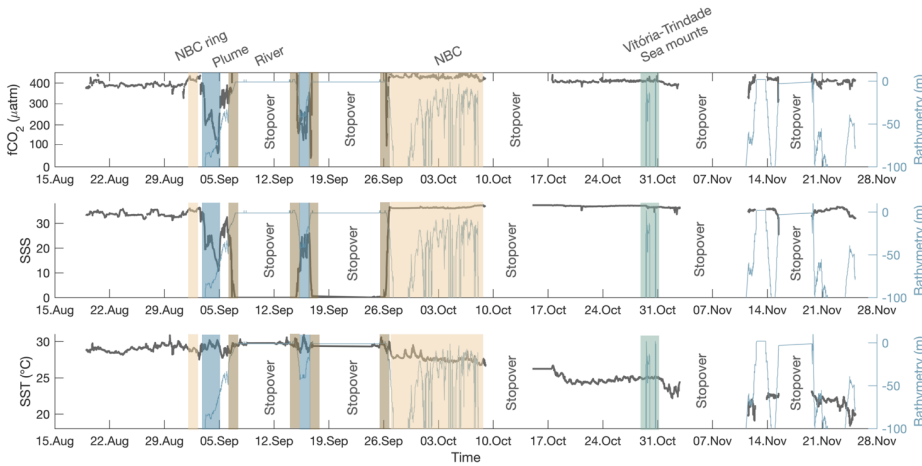
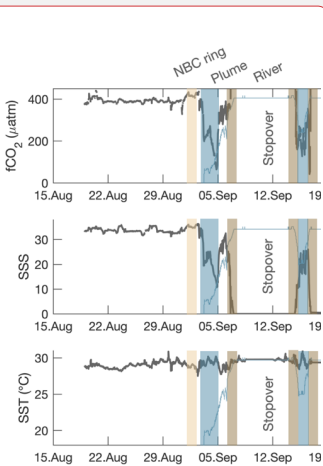


Figure 6: Time-series of fCO₂, sea surface salinity and sea surface temperature. The light blue line on each panel represents the along track ETOPO2v2 bathymetry. The shaded patches show areas of interest identified on Fig.1. NBC: North Brazil Current.



On 12 September, the schooner ~~left~~ the Amazon River and ~~sampl~~ed the Amazon and Pará Rivers plume before entering the Pará River to join Belém. The lowest fCO₂ of the time series ~~was~~ observed in the Amazon/ Pará River plume, with a fCO₂ of 42.8 µatm offshore of the Pará River. After the stopover in Belém, the ship ~~sampl~~ed the waters of the NBC. ~~The temperature decreased and showed a variability on the order of one degree Celsius. The NBC waters stand out by their high salinity (around 37) and high fCO₂ (~ 420 µatm), and strongly contrast with the river plume waters. From 9 October to 18 October the ship stopped in Salvador, and then sailed to Rio de Janeiro, with a particular focus on the Vitória-Trindade Seamounts, a biodiversity hotspot (Pinheiro et al., 2015) amidst the South Atlantic Subtropical Gyre, one of the most oligotrophic zones of the global ocean (Morel et al., 2010). The temperature was significantly colder (24°C after Salvador compared to 26/27°C before), and its variability is closely associated with the one of fCO₂ (the decrease in temperature is associated with a decrease in fCO₂ close to the rate of 4.23 %/°C given by Takahashi et al., 1993). This indicates a switch from a fCO₂ variability dominated by salinity and primary production to a fCO₂ variability dominated by a temperature solubility effect. Around the Vitória-Trindade Seamounts (28 October to 1 November) we observe a strong variability of surface salinity and CO₂, correlated to the shallower bathymetry, which could be driven by upwelling turbulent mixing (Mashayek et al., 2024; Napolitano et al., 2021).~~

The ship ~~called~~ in Rio de Janeiro from 2 November to 11 November and then ~~sailed~~ to Itajai with a call in Santos. This part of the journey is very coastal, with bottom depth almost always above 100 m. It shows strong fCO₂ variability, with low values associated to the ~~lower~~ salinities (34.8) close to Santos. After 19 November, the temperature ~~decreased~~ as the ship ~~sailed~~ southward ~~reaching~~ a minimum of 18.4 °C, associated to a small drop in fCO₂. Salinity also ~~decreased~~ to 31 as bottom ~~depths~~ ~~get~~ shallower than 50 m, possibly an early signal from the Rio de la Plata plume or/and a signal from the Lagoa dos Patos.

- a supprimé: leaves
- a supprimé: samples
- a supprimé: is
- a supprimé: samples
- a supprimé: They
- a supprimé: The temperature is decreasing and shows a variability on the order of one degree Celsius.
- a supprimé: stops
- a supprimé: da Bahia
- a supprimé: sails
- a supprimé: is
- a supprimé: It

Code de champ modifié

- a supprimé: calls
- a supprimé: sails
- a supprimé: low
- a supprimé: decreases
- a supprimé: sails
- a supprimé: and reaches
- a supprimé: decreases
- a supprimé: depth gets
- a supprimé: lagoa

3.2 The Amazon river-ocean continuum

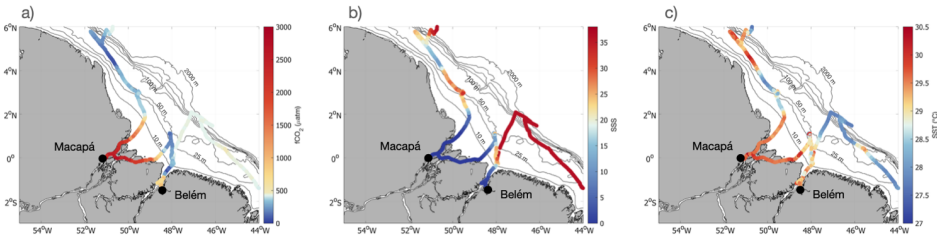
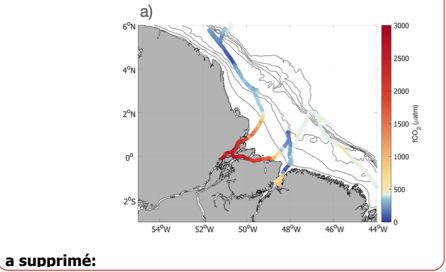


Figure 7: Along track fCO₂ (a), sea surface salinity (b) and sea surface temperature (c) in the Amazon region. Bathymetry contours are represented in black, from 10 m to 2000 m.

The largest variations of fCO₂ are observed in the AROC. The strongest gradient, reaching 3000 µatm, is observed at the transition between the ~~marine~~ and riverine waters. The signature of the ARP in itself is important, with a variation of fCO₂ of



- a supprimé: maritime

up to 340 μatm (Fig. 6). The minimum observed fCO_2 in the Amazon River plume is of 65 μatm (4.5°N/50.77°W), whereas outside of the plume, in the NBC, the fCO_2 is around 420 μatm . Then, on the Amazon shelf, fCO_2 progressively gets stronger as *Tara* went southward towards the Amazon estuary, with the change in regime intensifying around the 30 m bathymetry line, when the ARP switches from a sink to a very strong source ($\text{fCO}_2 > 2000 \mu\text{atm}$, Fig. 7). The AROC is sampled twice, and so is the Pará river-ocean continuum (Fig. 6, 7).

For the four crossings of the river-ocean continuum (two in the Amazon River, two in the Pará River), different fCO_2 /SSS relationships (Fig. 8) and different relationships to bathymetry (Fig. 9) are observed. From the NBC to the core of the ARP (6°N to 4°N, in dark blue on Fig. 8a, b), the fCO_2 /SSS measurements follow well the relationship reported in Lefèvre et al., (2010, then NL). However, when salinity and fCO_2 increase locally from 4°N to 2°N, (light blue and brown on Fig.8), they move away from the NL linear relationship. This is even more pronounced closer to the Amazon River, where the salinity decreases (from 25 to 0) and bottom depth is shallower than 20 m (Fig. 9). After a slow decrease for salinity ranging from 25 to 12, fCO_2 sharply increases in a non-linear fashion as the bathymetry gets shallower than 20 m (salinity ranging from 12 to 5). For depth shallower than 10 m and salinities below 5, the fCO_2 is already greater than 1000 μatm and shows the largest variability (on the order of 500 μatm) before the ship enters the pure riverine waters (0 salinity, depth of ~ 2 m, Fig. 8b, 9b).

a supprimé: In the center of the plume, the

a supprimé: .

a mis en forme : Police :Times New Roman

a supprimé: Table 1: Coordinates of each region defined on Figures 8 and 9. On Figure 8, regions 'Open Ocean to Belém' and 'Belém to open ocean' are merged. REGION

a supprimé: . Table 1

a supprimé: .

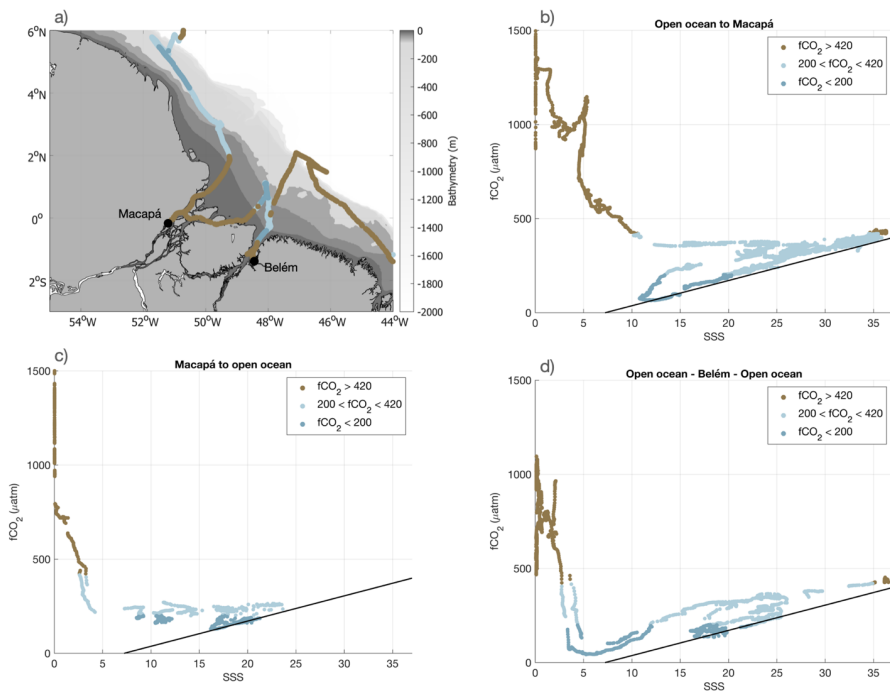
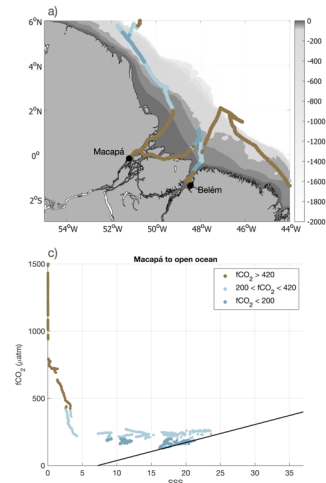


Figure 8: a) Map of the Amazon region, with bathymetry contours. Each region is defined on Figure 9. The track is colored based on the $f\text{CO}_2$ values to highlight three regimes ($f\text{CO}_2 > 420$ μatm (brown), $200\mu\text{atm} < f\text{CO}_2 < 420\mu\text{atm}$ (light blue) and $f\text{CO}_2 \leq 200$ μatm (dark blue)). $f\text{CO}_2$ -SSS diagram for the entrance in the Amazon River (b) for the exit of the Amazon River (c) and for the sampling of the Pará River (d). The black line on b) c) d) is the $f\text{CO}_2$ /SSS relationship from Lefèvre et al., (2010).

The schooner leaves the Amazon River through a different branch than on entry (Fig. 8a). The decrease in $f\text{CO}_2$ from 1000 μatm to 300 μatm is more linear with respect to salinity, and the source-sink transition occurs at a lower salinity than on entry (3 instead of 12, Fig. 8c). The points in the 5 to 25 salinity range show great variability, and only those with the lowest $f\text{CO}_2$ and salinities between 15 and 20 follow the NL relationship. The variation of salinity with bathymetry is not the same as in the way in, where the salinity stays lower than 15 for depths between 20 and 40 m.



a supprimé:

a supprimé: in table I

The variation of $f\text{CO}_2$ along the way in the Pará River is also different from the way out, but with less variability than for the Amazon River (Fig. 8d). The sink-source transition occurs at salinities of 2.7 and 3.7 respectively and for very shallow depth (< 5 m, Fig. 9a). The minimum $f\text{CO}_2$ reached before the Pará River is $42.7 \mu\text{atm}$ for a salinity of 5, whereas on the way out it is $101.6 \mu\text{atm}$ for a salinity of 7. This is likely due to the Pará River plume being advected northwestward along the shelf and mixing with the ARP on its northern side. On the southern side, it mixes with the carbon-rich waters of the NBC.

The transition from a source to a sink thus presents large variability. It doesn't happen at a consistent salinity or bottom depth, highlighting the role of other parameters driving the $f\text{CO}_2$ variability in the region.

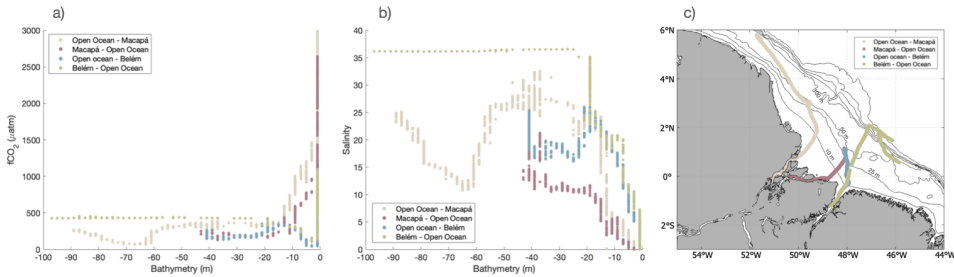


Figure 9: a) $f\text{CO}_2$ -bathymetry and b) SSS-bathymetry of the different river-ocean continuum crossings for depths shallower than 95 m. The bathymetry is ETOPO2v2 colocized along the ship track.

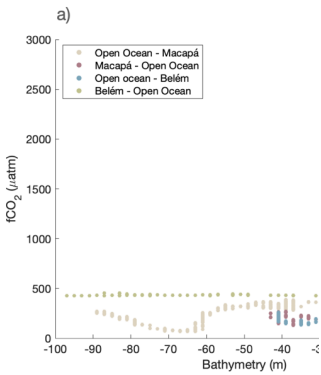
4 Discussion

4.1 Main drivers of $f\text{CO}_2$ variability

4.1.1 Salinity

In the equatorial band (15°N - 15°S) of the western Atlantic, the $f\text{CO}_2$ variability in the data follows well the strong surface salinity variability (Fig. 6). There are two reasons for that. First, in this region, the surface temperature is very warm ($\text{SST} > 27^\circ\text{C}$), with relatively small variability (the STD of the SST in the dataset is of 0.8°C). The solubility effect associated to an increase in temperature of 0.8°C would be an increase of the $f\text{CO}_2$ by $13.6 \mu\text{atm}$ (Takahashi et al. 1993, $4.23\%/^\circ\text{C}$). While this is non-negligible, it is small compared to the observed STD of $109 \mu\text{atm}$ observed in the *Tara* dataset between 15°N and 15°S (excluding waters with $\text{SSS} \leq 1$).

Second, the Amazon River flows into the tropical Atlantic and forms huge salinity gradients (STD of the SSS in the *Tara* dataset between 15°N and 15°S is of 7.5 (for $\text{SSS} > 1$)). These gradients indicate the river's influence on the open ocean, and thus also the changes in biogeochemical properties. At first order, the gradient in salinity is indicative the gradient in alkalinity



a supprimé:

a supprimé: tropical

a supprimé: and biological

555 and DIC (linked to biological activity) associated to the river plume and therefore fCO₂. This explains the robustness of
empirical linear relationships between salinity and fCO₂ in the ARP, such as the one of Lefèvre et al., (2010), presented in part
3.2.

4.1.2 Temperature

South of 15°S, the situation is different, with larger temperature changes. As the schooner sails poleward, the temperature
560 decreases with no more influence of the Amazon River system. At first order, the fCO₂ variations follow the one expected
from the solubility effect. The SST decreases of 8°C, and the change in fCO₂, with a maximum of 442.8 µatm and a minimum
of 309.2 µatm, is coherent with a drop of 8°C in temperature (expected drop in fCO₂ of 136 µatm following a 4.23 %/°C effect;
Takahashi et al., 1993).

Nevertheless, while the large-scale variability of the fCO₂ reflects the latitudinal temperature gradient (Landschützer et al.,
565 2013), at smaller scales the variability of salinity is also important and different water masses are sampled. Notably, south of
Rio de Janeiro, the schooner sails on the shelf, with a bathymetry often shallower than 100 m (Abril et al., 2022). Other river
discharges reach the south Atlantic, such as the one of the Rio de la Plata (Marta-Almeida et al., 2021). These waters spread
on the shelf and generate variability in salinity, suspended sediments and biological activity (Marta-Almeida et al., 2021; Piola
et al., 2005).

570

4.2 The sink-source transition in the river-ocean continuum

The multiple crossings of the river-ocean continuum show a great fCO₂ variability in the Amazon River/ Pará River estuaries
and resulting plumes on the Amazon shelf. As a continuous feature, this environment can extend over 500 km along-shelf and
200 km across-shelf (Curtin and Legeckis, 1986). Within this region, the transports of fresh water, sediment, nutrients and
575 biomass are determined by energetic processes occurring on semidiurnal, several-day, several-week and seasonal time scales
(Curtin, 1986; Geyer et al., 1991).

In the regions close to the river estuary, the fCO₂ changes are no longer primarily associated with the changes in salinity. As
580 salinity decreases, the switch from a decreasing fCO₂ (representative of the plume) to increasing fCO₂ (representative of the
river) does not happen at the same salinity for each crossing. Moreover, the linear relationship between salinity and fCO₂ does
not hold close to the river. It is thus likely that the salinity gradient no longer mirrors the gradient in DIC or in TA. The strong
sediment load of the Amazon River prevents the light penetration in the water column and the development of photosynthetic
organisms (DeMaster et al., 1986; Gagne-Maynard et al., 2017). The source to sink transition is mainly driven by the switch
585 from a respiration dominated system to a photosynthetic one (Gagne-Maynard et al., 2017; Mu et al., 2021). Several factors
impact the suspension of sediments in the water column and the development of phytoplankton, such as the bathymetry, winds,
intensity of the outflow (that can be influenced by large-scale climatic modes) and the tides (Gomes et al., 2021). Indeed, tides

a supprimé: The good agreement for a reasonable salinity range of this new dataset with the pre-existing relationship a further validation of the quality of the data.

a supprimé: .

a supprimé: . Other river discharges reach the south Atlantic, such as the one of the Rio de la Plata.

a supprimé: .

a supprimé: anymore. As salinity decreases, the switch from a decreasing fCO₂ (representative of the plume) to increasing fCO₂ (representative of the river) does not happen at the same salinity for each crossing. Moreover, the linear relationship between salinity and fCO₂ does not hold close to the river. It is thus likely that the salinity gradient no longer mirrors the gradient in DIC or in TA. The strong sediment load of the Amazon River prevents the light penetration in the water column and the development of photosynthetic organisms (DeMaster et al., 1986). The source to sink transition is mainly driven by the switch from a respiration dominated system to a photosynthetic one. Several factors impact the suspension of sediments in the water column and the development of phytoplankton, such as the bathymetry, winds and the tides. Indeed, tides and tidal currents are one of the dominant factors of the variability of the Amazon estuary with tidal currents ranging from 0.5 to 2.0 m s⁻¹ (Geyer et al., 1991)

610 and tidal currents are one of the dominant factors of the variability of the Amazon estuary with tidal currents ranging from 0.5 to 2.0 m s⁻¹ (Geyer et al., 1991; Ruault et al., 2020).

The relationship between suspended sediments and bathymetry allowed the identification of 4 zones of interactions by Curtin & Legeckis (1986). They match well with the fCO₂ measurements. For the Amazon River, the zone of highest suspended sediments concentration (SSC) is located between the isobaths 4 m and 11 m, matching the strong increase of the fCO₂ observed for the two crossings of the AROC. The zone of lowest SSC is between the isobaths 10 m and 20 m, associated to a diatom bloom in 1983 (Curtin and Legeckis, 1986; DeMaster et al., 1986). It is also the region where we observe the transition from a source to a sink of CO₂ (Fig. 9). For the Pará River, this region extends directly to the mouth, for depth shallower than 5 m. It also matches the observations, and the differences between the two rivers. Indeed, while for the Amazon River, the transition from a sink to a source happens between 10 and 20-m depth, it happens at much shallower depths for the Pará River (below 10 m). Their “River Zone”, for depth below 5 m, indeed corresponds to a salinity of 0. Nevertheless, we observe significant variability of fCO₂ even if the salinity does not change anymore. This region was not investigated by these studies that focused further offshore of the mouth. For the region, the bathymetry used here is not adapted anymore, and a specific Amazon estuary bathymetry should be used for further studies (such as Fassoni-Andrade et al., 2021). Therefore, combining the fCO₂ dataset and the numerous optical measurements also conducted underway onboard the *Tara* Mission Microbiome could lead to a better understanding of the AROC system. Moreover, linking this continuous dataset to the discrete imaging and genetic samples from Mission Microbiome’s stations, conducted in the different zones of the system, will also bring light on the biological communities responsible for the strong CO₂ source or sink observed.

4.3 Limitations of the dataset

Onboard *Tara*, there is rarely a trained scientist to take care of an equilibrator fCO₂ system. The system therefore has to run almost autonomously, and is monitored from land when someone trained is not onboard. Limited space meant that only two standards were used, and they were stored outside on the foredeck. The deck is subject to spray, waves and wave-related impacts. This increases the strain on the system, and the possibility of failure, in particularly during bad weather. The fCO₂ system operations were finally terminated due to several leakages that happened during the strong sea state encountered in the Southern Ocean. For this mission, *Tara* sampled mainly coastal environments, where CO₂ is highly variable and little known. There are very little previously acquired data in the region that can be used for comparison. And even where there are other data, the variability in the coastal ocean is such that it might not be comparable. Some surface samples of DIC and TA were collected by scientists on board, which were essential to validate the fCO₂ measured. The mean difference of 2 µatm and STD_{diff} of 7.4 µatm (going down to 0.5 µatm in the less variable environment) give an estimate of the uncertainty that support the validity of the dataset. It is nevertheless necessary to note that the relationship to compute fCO₂ from DIC and TA also has an uncertainty of 5.4 µatm, and it would be more accurate to cross-compare with fCO₂ measurements conducted in the same region at the same time as recommended by SOCAT. This shows the limitation of autonomous fCO₂ systems that cannot be

a supprimé: if they would exist

checked regularly, and especially the ones on small boats that are more fragile due to the rougher conditions than on a large research or container ship.

5 Conclusion

For the first time, a schooner equipped with a fCO₂ equilibrator system measured fCO₂ along the eastern coasts of South America. This high temporal resolution dataset includes fCO₂ measurements every minute over 14,000 km of sailing. From the Caribbean to Argentina, this 4-month dataset of 65,000 measurements (from August to ~~end of November~~ 2021) shows large fCO₂ variability with a standard deviation of 480 µatm. In particular, it sampled the Amazon River plume, the Amazon and Pará River estuaries, the North Brazil Current, the Brazil Current, the Vitória-Trindade Sea mounts (local hotspot of biodiversity), and the shelves of southern Brazil.

In August-September 2021, the Amazon-Pará plume is highly undersaturated with CO₂, in line with the many regional studies on the Amazon River plume (Ibáñez et al., 2015; Körtzinger, 2003; Lefèvre et al., 2010; Mu et al., 2021). This dataset provides data closer to the river than in some of these earlier studies, sampling the heart of the plume. Further from the mouth, fCO₂ reaches extreme low values, between 40 and 60 µatm, which had never been observed before. It is possible to measure such low values because for the first time a ship equipped with a fCO₂ system is sampling the river-ocean continuum, and pumping water at a very shallow depth. When salinity continues to drop (S<8), a sink-source transition occurs, and fCO₂ rises rapidly. The influence of the river becomes dominant, and fCO₂ reaches 3000 µatm in the river. The river-ocean continuum has been crossed four times, and each time showed different properties. This system is highly dynamic and needs to be studied further in depth to infer the global role of the Amazon system in the global carbon budget.

Equipping a sailboat with a fCO₂ equilibrator system is a challenge, but one that has been met by the schooner *Tara*. The dataset is very valuable for global and regional studies, ~~providing data in the data-poor region of the~~ coastal regions of the South Atlantic Ocean. It is particularly helpful for fCO₂ mapping products, which assimilate all data collected to produce global monthly and climatological fCO₂ maps from neural network reconstruction (Chau et al., 2024; Denvil-Sommer et al., 2019; Landschützer et al., 2016, 2020; Laruelle et al., 2017). It is also useful for process studies, such as the river-ocean continuum (Sawakuchi et al., 2017), offshore ARP (Olivier et al., 2024b), ~~and the coastal currents of the South American coast.~~ ~~The difficulty in validating the dataset shows just how little is known about coastal regions and how dynamic they are. The limited number of observations could be due to the complicated access some of these regions (distance from major port) and to the difficulty to obtain sampling permits.~~ Despite sampling most of the American coastline along the South Atlantic Ocean, it represents only a small fraction of the world’s coastlines. Collecting more fCO₂ data in under-sampled regions, such as the

a supprimé: December

a mis en forme : Indice

a supprimé: filling part of the

a supprimé: gap

a mis en forme : Indice

a mis en forme : Indice

a supprimé: , the Guanabara Bay (Cotovicz Jr et al., 2015), and the coastal currents of the South American coast. The difficulty in validating the dataset shows just how little is known about coastal regions and how dynamic they are.

southern hemisphere oceans, the Southern Ocean, coastal regions and estuaries, is very important to improve our knowledge of the global carbon cycle (Roobaert et al., 2019).

Data availability

685 The dataset is available in the following public repository: <https://doi.org/10.5281/zenodo.13790065> (Olivier et al., 2024a),
with the DOI 10.5281/zenodo.13790065. It is also submitted to the SOCAT version 2025.

a mis en forme : Police :+Corps (Times New Roman), 10 pt
a mis en forme : Police :+Corps (Times New Roman), 10 pt

Author contribution

LO, JB and GR conceptualized the project. LO, TL, NH and AC collected the data and LO and CH curated the data. CH and
690 DV designed and provided the instrument to collect the dataset. SP managed and coordinated the project on land and on board
for the mission. LO prepared the manuscript with contributions from all co-authors.

Competing interests

The authors declare that they have no conflict of interest.

695

Acknowledgements

We wish to thank the Tara Ocean Foundation, the SV *Tara* crew and all those who participate in Mission Microbiomes
AtlantECO and adopt its Data Sharing & Publication Best Practices(<https://zenodo.org/communities/mission-microbiomes-atlanteco/>). In particular, we would like to thank chief engineer Léo Boulon for all his help with the installation of the system
700 as well as Martin Hertau, Nicolas Bin and Samuel Audrain for the maintenance. Clémentine Moulin and Aliénor Bourdais,
thank you for the help with the logistics, the shipping and the coordination. We warmly thank the SNAPOCO₂ and Jonathan
Fin for the precious accurate analysis of the DIC/TA samples. We are keen to thank the commitment of the following
institutions for their financial and scientific support that made Mission Microbiomes AtlantECO possible: Stazione Zoologica
Anton Dohrn, European Bioinformatics Institute (EMBL-EBI), Centre national de la recherche scientifique (CNRS), Centre
705 National de Séquençage (CNS, Genoscope), agnès b., BIC, Capgemini Engineering, Fondation Groupe EDF, Compagnie
Nationale du Rhône, L'Oréal, Biotherm, Région Bretagne, Lorient Agglomération, Billerudkorsnas, Havas Paris, Fondation
Rothschild, Office Français de la Biodiversité, AmerisourceBergen, Philgood Foundation, UNESCO-IOC, Etienne Bourgois.

Financial support

710 This publication has received funding from the European Union's Horizon 2020 research and innovation programme under
grant agreement No 862923 (project AtlantECO). This output reflects only the author's view and the European Union cannot
be held responsible for any use that may be made of the information contained therein. This work was supported by the
Initiative and Networking Fund of the Helmholtz Association (Grant Number: VH-NG-19-33). P.C.J. was supported by

Fundação de Amparo à Pesquisa do Estado de São Paulo (FAPESP; PhD grant no. 2017/26786-1) and by FAI/UFSCar (ProEx no. 3213/2020-83) through the European Union—H2020 project AtlantECO (award no. 862923).

References

- Abril, G., C. Cotoviez Jr., L. Nepomuceno, A., Erbas, T., Costa, S., V. Ramos, V., Moser, G., Fernandes, A., Negri, E., A. Knoppers, B., Brandini, N., Machado, W., Bernardes, M., and Vantrepotte, V.: SPREADING EUTROPHICATION AND CHANGING CO₂ FLUXES IN THE TROPICAL COASTAL OCEAN: A FEW LESSONS FROM RIO DE JANEIRO. *Arq. Ciênc. Mar.*, 55, 461–476, <https://doi.org/10.32360/acmar.v55iEspecial.78518>, 2022.
- Andrié, C., Oudot, C., Genthon, C., and Merlivat, L.: CO₂ fluxes in the tropical Atlantic during FOCAL cruises, *J. Geophys. Res. Oceans*, 91, 11741–11755, <https://doi.org/10.1029/JC091iC10p11741>, 1986.
- Araujo, M., Noriega, C., Hounsou-gbo, G. A., Velela, D., Araujo, J., Bruto, L., Feitosa, F., Flores-Montes, M., Lefèvre, N., Melo, P., Otsuka, A., Travassos, K., Schwamborn, R., and Neumann-Leitão, S.: A Synoptic Assessment of the Amazon River-Ocean Continuum during Boreal Autumn: From Physics to Plankton Communities and Carbon Flux, *Front. Microbiol.*, 8, 2017.
- Bakker, D. C. E., Pfeil, B., Landa, C. S., Metzl, N., O'Brien, K. M., Olsen, A., Smith, K., Cosca, C., Harasawa, S., Jones, S. D., Nakaoka, S., Nojiri, Y., Schuster, U., Steinhoff, T., Sweeney, C., Takahashi, T., Tilbrook, B., Wada, C., Wanninkhof, R., Alin, S. R., Balestrini, C. F., Barbero, L., Bates, N. R., Bianchi, A. A., Bonou, F., Boutin, J., Bozec, Y., Burger, E. F., Cai, W.-J., Castle, R. D., Chen, L., Chierici, M., Currie, K., Evans, W., Featherstone, C., Feely, R. A., Fransson, A., Goyet, C., Greenwood, N., Gregor, L., Hankin, S., Hardman-Mountford, N. J., Harlay, J., Hauck, J., Hoppema, M., Humphreys, M. P., Hunt, C. W., Huss, B., Ibáñez, J. S. P., Johannessen, T., Keeling, R., Kitidis, V., Körtzinger, A., Kozyr, A., Krasakopoulou, E., Kuwata, A., Landschützer, P., Lauvset, S. K., Lefèvre, N., Lo Monaco, C., Manke, A., Mathis, J. T., Merlivat, L., Millero, F. J., Monteiro, P. M. S., Munro, D. R., Murata, A., Newberger, T., Omar, A. M., Ono, T., Paterson, K., Pearce, D., Pierrot, D., Robbins, L. L., Saito, S., Salisbury, J., Schlitzer, R., Schneider, B., Schweitzer, R., Sieger, R., Skjelvan, I., Sullivan, K. F., Sutherland, S. C., Sutton, A. J., Tadokoro, K., Telszewski, M., Tuma, M., van Heuven, S. M. A. C., Vandemark, D., Ward, B., Watson, A. J., and Xu, S.: A multi-decade record of high-quality *f*CO₂ data in version 3 of the Surface Ocean CO₂ Atlas (SOCAT), *Earth Syst. Sci. Data*, 8, 383–413, <https://doi.org/10.5194/essd-8-383-2016>, 2016.
- Bauer, J. E., Cai, W.-J., Raymond, P. A., Bianchi, T. S., Hopkinson, C. S., and Regnier, P. A. G.: The changing carbon cycle of the coastal ocean, *Nature*, 504, 61–70, <https://doi.org/10.1038/nature12857>, 2013.
- Borges, A. V.: Do we have enough pieces of the jigsaw to integrate CO₂ fluxes in the coastal ocean?, *Estuaries*, 28, 3–27, <https://doi.org/10.1007/BF02732750>, 2005.
- Bork, P., Bowler, C., de Vargas, C., Gorsky, G., Karsenti, E., and Wincker, P.: Tara Oceans studies plankton at planetary scale, *Science*, 348, 873–873, <https://doi.org/10.1126/science.aac5605>, 2015.
- Cai, W.-J., Dai, M., and Wang, Y.: Air-sea exchange of carbon dioxide in ocean margins: A province-based synthesis,

- Geophys. Res. Lett., 33, <https://doi.org/10.1029/2006GL026219>, 2006.
- Chau, T.-T.-T., Gehlen, M., Metzl, N., and Chevallier, F.: CMEMS-LSCE: a global, 0.25°, monthly reconstruction of the surface ocean carbonate system, *Earth Syst. Sci. Data*, 16, 121–160, <https://doi.org/10.5194/essd-16-121-2024>, 2024.
- Chen, C.-T. A., Huang, T.-H., Chen, Y.-C., Bai, Y., He, X., and Kang, Y.: Air–sea exchanges of CO₂ in the world’s coastal
750 seas, *Biogeosciences*, 10, 6509–6544, <https://doi.org/10.5194/bg-10-6509-2013>, 2013.
- Cooley, S. R., Coles, V. J., Subramaniam, A., and Yager, P. L.: Seasonal variations in the Amazon plume-related atmospheric carbon sink: SEASONALITY OF CO₂ IN AMAZON PLUME, *Glob. Biogeochem. Cycles*, 21, n/a-n/a, <https://doi.org/10.1029/2006GB002831>, 2007.
- Cotovicz Jr, L. C., Knoppers, B. A., Brandini, N., Costa Santos, S. J., and Abril, G.: A strong CO₂ sink enhanced by
755 eutrophication in a tropical coastal embayment (Guanabara Bay, Rio de Janeiro, Brazil), *Biogeosciences*, 12, 6125–6146, 2015.
- Curtin, T. B.: Physical observations in the plume region of the Amazon River during peak discharge—II. Water masses, *Cont. Shelf Res.*, 6, 53–71, [https://doi.org/10.1016/0278-4343\(86\)90053-1](https://doi.org/10.1016/0278-4343(86)90053-1), 1986.
- Curtin, T. B. and Legeckis, R. V.: Physical observations in the plume region of the Amazon River during peak discharge—I. Surface variability, *Cont. Shelf Res.*, 6, 31–51, [https://doi.org/10.1016/0278-4343\(86\)90052-X](https://doi.org/10.1016/0278-4343(86)90052-X), 1986.
- 760 Dai, A. and Trenberth, K. E.: Estimates of Freshwater Discharge from Continents: Latitudinal and Seasonal Variations, *J. Hydrometeorol.*, 3, 660–687, [https://doi.org/10.1175/1525-7541\(2002\)003<0660:EOFDFC>2.0.CO;2](https://doi.org/10.1175/1525-7541(2002)003<0660:EOFDFC>2.0.CO;2), 2002.
- DeMaster, D. J., Kuehl, S. A., and Nittrouer, C. A.: Effects of suspended sediments on geochemical processes near the mouth of the Amazon River: examination of biological silica uptake and the fate of particle-reactive elements, *Cont. Shelf Res.*, 6, 107–125, [https://doi.org/10.1016/0278-4343\(86\)90056-7](https://doi.org/10.1016/0278-4343(86)90056-7), 1986.
- 765 Denvil-Sommer, A., Gehlen, M., Vrac, M., and Mejia, C.: LSCE-FFNN-v1: a two-step neural network model for the reconstruction of surface ocean *p*CO₂ over the global ocean, *Geosci. Model Dev.*, 12, 2091–2105, <https://doi.org/10.5194/gmd-12-2091-2019>, 2019.
- Dickson, A. G.: Guide to best practices for ocean CO₂ measurements, *PICES Spec. Publ.*, 191, 2007.
- Dickson, A. G. and Millero, F. J.: A comparison of the equilibrium constants for the dissociation of carbonic acid in seawater
770 media, *Deep Sea Res. Part Oceanogr. Res. Pap.*, 34, 1733–1743, [https://doi.org/10.1016/0198-0149\(87\)90021-5](https://doi.org/10.1016/0198-0149(87)90021-5), 1987.
- [Dong, Y., Bakker, D. C. E., and Landschützer, P.: Accuracy of Ocean CO₂ Uptake Estimates at a Risk by a Reduction in the Data Collection, *Geophys. Res. Lett.*, 51, e2024GL108502, <https://doi.org/10.1029/2024GL108502>, 2024.](#)
- [Fassoni-Andrade, A. C., Durand, F., Moreira, D., Azevedo, A., dos Santos, V. F., Funi, C., and Laraque, A.: Comprehensive bathymetry and intertidal topography of the Amazon estuary, *Earth Syst. Sci. Data*, 13, 2275–2291, <https://doi.org/10.5194/essd-13-2275-2021>, 2021.](#)
- 775 [Friedlingstein, P., O’Sullivan, M., Jones, M. W., Andrew, R. M., Bakker, D. C. E., Hauck, J., Landschützer, P., Le Quéré, C., Luijkx, I. T., Peters, G. P., Peters, W., Pongratz, J., Schwingshackl, C., Sitch, S., Canadell, J. G., Ciais, P., Jackson, R. B., Alin, S. R., Anthoni, P., Barbero, L., Bates, N. R., Becker, M., Bellouin, N., Decharme, B., Bopp, L., Brasika, I. B. M., Cadule, P., Chamberlain, M. A., Chandra, N., Chau, T.-T.-T., Chevallier, F., Chini, L. P., Cronin, M., Dou, X., Enyo, K., Evans, W.,](#)

780 Falk, S., Feely, R. A., Feng, L., Ford, D. J., Gasser, T., Ghattas, J., Gkritzalis, T., Grassi, G., Gregor, L., Gruber, N., Gürses, Ö., Harris, I., Hefner, M., Heinke, J., Houghton, R. A., Hurtt, G. C., Iida, Y., Ilyina, T., Jacobson, A. R., Jain, A., Jarníková, T., Jersild, A., Jiang, F., Jin, Z., Joos, F., Kato, E., Keeling, R. F., Kennedy, D., Klein Goldewijk, K., Knauer, J., Korsbakken, J. I., Körtzinger, A., Lan, X., Lefèvre, N., Li, H., Liu, J., Liu, Z., Ma, L., Marland, G., Mayot, N., McGuire, P. C., McKinley, G. A., Meyer, G., Morgan, E. J., Munro, D. R., Nakaoka, S.-I., Niwa, Y., O'Brien, K. M., Olsen, A., Omar, A. M., Ono, T.,

785 Paulsen, M., Pierrot, D., Pocock, K., Poulter, B., Powis, C. M., Rehder, G., Resplandy, L., Robertson, E., Rödenbeck, C., Rosan, T. M., Schwinger, J., Séférian, R., et al.: Global Carbon Budget 2023, *Earth Syst. Sci. Data*, 15, 5301–5369, <https://doi.org/10.5194/essd-15-5301-2023>, 2023.

[Gagne-Maynard, W. C., Ward, N. D., Keil, R. G., Sawakuchi, H. O., Da Cunha, A. C., Neu, V., Brito, D. C., Da Silva Less, D. F., Diniz, J. E. M., De Matos Valerio, A., Kampel, M., Krusche, A. V., and Richey, J. E.: Evaluation of Primary Production in the Lower Amazon River Based on a Dissolved Oxygen Stable Isotopic Mass Balance, *Front. Mar. Sci.*, 4, <https://doi.org/10.3389/fmars.2017.00026>, 2017.](#)

790 Geyer, W. R., Beardsley, R. C., Candela, J., Castro, B. M., Legeckis, R. V., Lentz, S. J., Limeburner, R., Miranda, L. B., and Trowbridge, J. H.: The physical oceanography of the Amazon outflow, *Oceanography*, 4, 8–14, 1991.

[Gomes, V. J. C., Asp, N. E., Siegle, E., Gomes, J. D., Silva, A. M. M., Ogston, A. S., and Nittrouer, C. A.: Suspended-Sediment Distribution Patterns in Tide-Dominated Estuaries on the Eastern Amazon Coast: Geomorphic Controls of Turbidity-Maxima Formation, *Water*, 13, 1568, <https://doi.org/10.3390/w13111568>, 2021.](#)

795 Ho, D. T. and Schanze, J. J.: Precipitation-induced reduction in surface ocean pCO₂: Observations from the eastern tropical Pacific Ocean, *Geophys. Res. Lett.*, 47, e2020GL088252, 2020.

Ibáñez, J. S. P., Diverres, D., Araujo, M., and Lefèvre, N.: Seasonal and interannual variability of sea-air CO₂ fluxes in the tropical Atlantic affected by the Amazon River plume, *Glob. Biogeochem. Cycles*, 29, 1640–1655, <https://doi.org/10.1002/2015GB005110>, 2015.

800 [Ibáñez, J. S. P., Araujo, M., and Lefèvre, N.: The overlooked tropical oceanic CO₂ sink, *Geophys. Res. Lett.*, 43, 3804–3812, <https://doi.org/10.1002/2016GL068020>, 2016.](#)

Körtzinger, A.: A significant CO₂ sink in the tropical Atlantic Ocean associated with the Amazon River plume, *Geophys. Res. Lett.*, 30, <https://doi.org/10.1029/2003GL018841>, 2003.

805 Landschützer, P., Gruber, N., [Bakker, D. C. E., Schuster, U., Nakaoka, S., Payne, M. R., Sasse, T. P., and Zeng, J.: A neural network-based estimate of the seasonal to inter-annual variability of the Atlantic Ocean carbon sink, *Biogeosciences*, 10, 7793–7815, <https://doi.org/10.5194/bg-10-7793-2013>, 2013.](#)

[Landschützer, P., Gruber, N., and Bakker, D. C. E.: Decadal variations and trends of the global ocean carbon sink, *Glob. Biogeochem. Cycles*, 30, 1396–1417, <https://doi.org/10.1002/2015GB005359>, 2016.](#)

810 Landschützer, P., Laruelle, G. G., Roobaert, A., and Regnier, P.: A uniform pCO₂ climatology combining open and coastal oceans, *Earth Syst. Sci. Data*, 12, 2537–2553, <https://doi.org/10.5194/essd-12-2537-2020>, 2020.

Landschützer, P., Tanhua, T., Behncke, J., and Keppler, L.: Sailing through the southern seas of air–sea CO₂ flux uncertainty,

Philos. Trans. R. Soc. Math. Phys. Eng. Sci., 381, 20220064, <https://doi.org/10.1098/rsta.2022.0064>, 2023.

a mis en forme : Français

815 Laruelle, G. G., Lauerwald, R., Pfeil, B., and Regnier, P.: Regionalized global budget of the CO₂ exchange at the air-water interface in continental shelf seas, *Glob. Biogeochem. Cycles*, 28, 1199–1214, <https://doi.org/10.1002/2014GB004832>, 2014.
Laruelle, G. G., Landschützer, P., Gruber, N., Tison, J.-L., Delille, B., and Regnier, P.: Global high-resolution monthly *p*CO₂ climatology for the coastal ocean derived from neural network interpolation, *Biogeosciences*, 14, 4545–4561, <https://doi.org/10.5194/bg-14-4545-2017>, 2017.

820 Lefèvre, N., Diverrès, D., and Gallois, F.: Origin of CO₂ undersaturation in the western tropical Atlantic, *Tellus B Chem. Phys. Meteorol.*, 62, 595–607, <https://doi.org/10.1111/j.1600-0889.2010.00475.x>, 2010.

Lefèvre, N., Flores Montes, M., Gaspar, F. L., Rocha, C., Jiang, S., De Araújo, M. C., and Ibáñez, J. S. P.: Net Heterotrophy in the Amazon Continental Shelf Changes Rapidly to a Sink of CO₂ in the Outer Amazon Plume, *Front. Mar. Sci.*, 4, 2017.

Lueker, T. J., Dickson, A. G., and Keeling, C. D.: Ocean *p*CO₂ calculated from dissolved inorganic carbon, alkalinity, and equations for K₁ and K₂: validation based on laboratory measurements of CO₂ in gas and seawater at equilibrium, *Mar. Chem.*, 70, 105–119, [https://doi.org/10.1016/S0304-4203\(00\)00022-0](https://doi.org/10.1016/S0304-4203(00)00022-0), 2000.

Marta-Almeida, M., Dalbosco, A., Franco, D., and Ruiz-Villarreal, M.: Dynamics of river plumes in the South Brazilian Bight and South Brazil, *Ocean Dyn.*, 71, 59–80, <https://doi.org/10.1007/s10236-020-01397-x>, 2021.

830 Mashayek, A., Gula, J., Baker, L. E., Naveira Garabato, A. C., Cimoli, L., Riley, J. J., and de Lavergne, C.: On the role of seamounts in upwelling deep-ocean waters through turbulent mixing, *Proc. Natl. Acad. Sci.*, 121, e2322163121, 2024.

Mayorga, E., Aufdenkampe, A. K., Masiello, C. A., Krusche, A. V., Hedges, J. I., Quay, P. D., Richey, J. E., and Brown, T. A.: Young organic matter as a source of carbon dioxide outgassing from Amazonian rivers, *Nature*, 436, 538–541, 2005.

Mehrbach, C., Culberson, C. H., Hawley, J. E., and Pytkowicz, R. M.: Measurement of the Apparent Dissociation Constants of Carbonic Acid in Seawater at Atmospheric Pressure, *Limnol. Oceanogr.*, 18, 897–907, <https://doi.org/10.4319/lo.1973.18.6.0897>, 1973.

835 Metzl, N., Fin, J., Lo Monaco, C., Mignon, C., Alliouane, S., Antoine, D., Bourdin, G., Boutin, J., Bozec, Y., Conan, P., Coppola, L., Diaz, F., Douville, E., Durrieu de Madron, X., Gattuso, J.-P., Gazeau, F., Golbol, M., Lansard, B., Lefèvre, D., Lefèvre, N., Lombard, F., Louanchi, F., Merlivat, L., Olivier, L., Petrenko, A., Petton, S., Pujo-Pay, M., Rabouille, C., Reverdin, G., Ridame, C., Tribollet, A., Vellucci, V., Wagener, T., and Wimart-Rousseau, C.: A synthesis of ocean total alkalinity and dissolved inorganic carbon measurements from 1993 to 2022: the SNAPO-CO₂-v1 dataset, *Earth Syst. Sci. Data*, 16, 89–120, <https://doi.org/10.5194/essd-16-89-2024>, 2024.

Monteiro, T., Batista, M., Henley, S., Machado, E. da C., Araujo, M., and Kerr, R.: Contrasting Sea-Air CO₂ Exchanges in the Western Tropical Atlantic Ocean, *Glob. Biogeochem. Cycles*, 36, e2022GB007385, <https://doi.org/10.1029/2022GB007385>, 2022.

845 Morel, A., Claustre, H., and Gentili, B.: The most oligotrophic subtropical zones of the global ocean: similarities and differences in terms of chlorophyll and yellow substance, *Biogeosciences*, 7, 3139–3151, <https://doi.org/10.5194/bg-7-3139-2010>, 2010.

Mu, L., Gomes, H. do R., Burns, S. M., Goes, J. I., Coles, V. J., Rezende, C. E., Thompson, F. L., Moura, R. L., Page, B., and Yager, P. L.: Temporal Variability of Air-Sea CO₂ flux in the Western Tropical North Atlantic Influenced by the Amazon River Plume, *Glob. Biogeochem. Cycles*, 35, e2020GB006798, <https://doi.org/10.1029/2020GB006798>, 2021.

Napolitano, D. C., da Silveira, I. C. A., Tandon, A., and Calil, P. H. R.: Submesoscale Phenomena Due to the Brazil Current Crossing of the Vitória-Trindade Ridge, *J. Geophys. Res. Oceans*, 126, e2020JC016731, <https://doi.org/10.1029/2020JC016731>, 2021.

Olivier, L., Boutin, J., Reverdin, G., Lefèvre, N., Landschützer, P., Speich, S., Karstensen, J., Labaste, M., Noisel, C., Ritschel, M., Steinhoff, T., and Wanninkhof, R.: Wintertime process study of the North Brazil Current rings reveals the region as a larger sink for CO₂ than expected, *Biogeosciences*, 19, 2969–2988, <https://doi.org/10.5194/bg-19-2969-2022>, 2022.

Olivier, L., Reverdin, G., Boutin, J., Hunt, C., Linkowski, T., Chase, A. P., Haentjens, N., Junger, P. C., Pesant, S., and Vandemark, D.: CO₂ fugacity aboard the schooner Tara during Mission Microbiomes AtlantECO., <https://doi.org/10.5281/zenodo.13790064>, 2024a.

Olivier, L., Reverdin, G., Boutin, J., Laxenaire, R., Iudicone, D., Pesant, S., Calil, P. H. R., Horstmann, J., Couet, D., Erta, J. M., Huber, P., Sarmento, H., Freire, A., Koch-Larrouy, A., Vergely, J.-L., Rousselot, P., and Speich, S.: Late summer northwestward Amazon plume pathway under the action of the North Brazil Current rings, *Remote Sens. Environ.*, 307, 114165, <https://doi.org/10.1016/j.rse.2024.114165>, 2024b.

Pesant, S., Not, F., Picheral, M., Kandels-Lewis, S., Le Bescot, N., Gorsky, G., Iudicone, D., Karsenti, E., Speich, S., Troublé, R., Dimier, C., and Searson, S.: Open science resources for the discovery and analysis of Tara Oceans data, *Sci. Data*, 2, 150023, <https://doi.org/10.1038/sdata.2015.23>, 2015.

Pierrot, D., Neill, C., Sullivan, K., Castle, R., Wanninkhof, R., Lüger, H., Johannessen, T., Olsen, A., Feely, R. A., and Cosca, C. E.: Recommendations for autonomous underway pCO₂ measuring systems and data-reduction routines, *Deep Sea Res. Part II Top. Stud. Oceanogr.*, 56, 512–522, <https://doi.org/10.1016/j.dsr2.2008.12.005>, 2009.

Pinheiro, H. T., Mazzei, E., Moura, R. L., Amado-Filho, G. M., Carvalho-Filho, A., Braga, A. C., Costa, P. A. S., Ferreira, B. P., Ferreira, C. E. L., Floeter, S. R., Francini-Filho, R. B., Gasparini, J. L., Macieira, R. M., Martins, A. S., Olavo, G., Pimentel, C. R., Rocha, L. A., Sazima, I., Simon, T., Teixeira, J. B., Xavier, L. B., and Joyeux, J.-C.: Fish Biodiversity of the Vitória-Trindade Seamount Chain, Southwestern Atlantic: An Updated Database, *PLOS ONE*, 10, e0118180, <https://doi.org/10.1371/journal.pone.0118180>, 2015.

Piola, A. R., Matano, R. P., Palma, E. D., Möller Jr, O. O., and Campos, E. J.: The influence of the Plata River discharge on the western South Atlantic shelf, *Geophys. Res. Lett.*, 32, 2005.

Richey, J. E., Melack, J. M., Aufdenkampe, A. K., Ballester, V. M., and Hess, L. L.: Outgassing from Amazonian rivers and wetlands as a large tropical source of atmospheric CO₂, *Nature*, 416, 617–620, <https://doi.org/10.1038/416617a>, 2002.

Roobaert, A., Laruelle, G. G., Landschützer, P., Gruber, N., Chou, L., and Regnier, P.: The Spatiotemporal Dynamics of the Sources and Sinks of CO₂ in the Global Coastal Ocean, *Glob. Biogeochem. Cycles*, 33, 1693–1714, <https://doi.org/10.1029/2019GB006239>, 2019.

Ruault, V., Jouanno, J., Durand, F., Chanut, J., and Benshila, R.: Role of the Tide on the Structure of the Amazon Plume: A Numerical Modeling Approach, *J. Geophys. Res. Oceans*, 125, e2019JC015495, <https://doi.org/10.1029/2019JC015495>, 2020.

Sawakuchi, H. O., Neu, V., Ward, N. D., Barros, M. de L. C., Valerio, A. M., Gagne-Maynard, W., Cunha, A. C., Less, D. F. S., Diniz, J. E. M., Brito, D. C., Krusche, A. V., and Richey, J. E.: Carbon Dioxide Emissions along the Lower Amazon River, *Front. Mar. Sci.*, 4, 2017.

Sharp, J. D., Pierrot, D., Humphreys, M. P., Epitalon, J.-M., Orr, J. C., Lewis, E. R., and Wallace, D. W. R.: CO2SYSv3 for MATLAB, , <https://doi.org/10.5281/zenodo.4023039>, 2020.

Subramaniam, A., Yager, P. L., Carpenter, E. J., Mahaffey, C., Björkman, K., Cooley, S., Kustka, A. B., Montoya, J. P., Sañudo-Wilhelmy, S. A., Shipe, R., and Capone, D. G.: Amazon River enhances diazotrophy and carbon sequestration in the tropical North Atlantic Ocean, *Proc. Natl. Acad. Sci.*, 105, 10460–10465, <https://doi.org/10.1073/pnas.0710279105>, 2008.

Takahashi, T., Olafsson, J., Goddard, J. G., Chipman, D. W., and Sutherland, S. C.: Seasonal variation of CO₂ and nutrients in the high-latitude surface oceans: A comparative study, *Glob. Biogeochem. Cycles*, 7, 843–878, <https://doi.org/10.1029/93GB02263>, 1993.

Takahashi, T., Sutherland, S. C., Sweeney, C., Poisson, A., Metzl, N., Tilbrook, B., Bates, N., Wanninkhof, R., Feely, R. A., Sabine, C., Olafsson, J., and Nojiri, Y.: Global sea–air CO₂ flux based on climatological surface ocean pCO₂, and seasonal biological and temperature effects, *Deep Sea Res. Part II Top. Stud. Oceanogr.*, 49, 1601–1622, [https://doi.org/10.1016/S0967-0645\(02\)00003-6](https://doi.org/10.1016/S0967-0645(02)00003-6), 2002.

Tennekes, H.: The Logarithmic Wind Profile, *J. Atmospheric Sci.*, 30, 234–238, [https://doi.org/10.1175/1520-0469\(1973\)030<0234:TLWP>2.0.CO;2](https://doi.org/10.1175/1520-0469(1973)030<0234:TLWP>2.0.CO;2), 1973.

Valerio, A. de M., Kampel, M., Vantrepotte, V., Ward, N. D., Sawakuchi, H. O., Less, D. F. D. S., Neu, V., Cunha, A., and Richey, J.: Using CDOM optical properties for estimating DOC concentrations and pCO₂ in the Lower Amazon River, *Opt. Express*, 26, A657–A677, <https://doi.org/10.1364/OE.26.00A657>, 2018.

Vandemark, D., Salisbury, J. E., Hunt, C. W., Shellito, S. M., Irish, J. D., McGillis, W. R., Sabine, C. L., and Maenner, S. M.: Temporal and spatial dynamics of CO₂ air-sea flux in the Gulf of Maine, *J. Geophys. Res. Oceans*, 116, <https://doi.org/10.1029/2010JC006408>, 2011.

Ward, N. D., Keil, R. G., Medeiros, P. M., Brito, D. C., Cunha, A. C., Dittmar, T., Yager, P. L., Krusche, A. V., and Richey, J. E.: Degradation of terrestrially derived macromolecules in the Amazon River, *Nat. Geosci.*, 6, 530–533, 2013.

Ward, N. D., Krusche, A. V., Sawakuchi, H. O., Brito, D. C., Cunha, A. C., Moura, J. M. S., da Silva, R., Yager, P. L., Keil, R. G., and Richey, J. E.: The compositional evolution of dissolved and particulate organic matter along the lower Amazon River—Óbidos to the ocean, *Mar. Chem.*, 177, 244–256, 2015.

Ward, N. D., Bianchi, T. S., Medeiros, P. M., Seidel, M., Richey, J. E., Keil, R. G., and Sawakuchi, H. O.: Where Carbon Goes When Water Flows: Carbon Cycling across the Aquatic Continuum, *Front. Mar. Sci.*, 4, <https://doi.org/10.3389/fmars.2017.00007>, 2017.

Waters, J., Millero, F. J., and Woosley, R. J.: Corrigendum to “The free proton concentration scale for seawater pH”,

[MARCHE: 149 (2013) 8–22], Mar. Chem., 165, 66–67, <https://doi.org/10.1016/j.marchem.2014.07.004>, 2014.

